A Pathogenic Deletion in Forkhead Box L1 (FOXL1) Identifies the First Otosclerosis (OTSC) Gene

Nelly Abdelfatah
Memorial University of Newfoundland Faculty of Medicine
Ahmed A. Mostafa
Memorial University of Newfoundland Faculty of Medicine
Curtis R. French
Memorial University of Newfoundland Faculty of Medicine
Lance P. Doucette
Memorial University of Newfoundland Faculty of Medicine
Cindy Penney
Memorial University of Newfoundland Faculty of Medicine
Matthew B. Lucas
Western University
Anne Griffin
Memorial University of Newfoundland Faculty of Medicine
Valerie Booth
Memorial University of Newfoundland Faculty of Science
Christopher Rowley
Memorial University of Newfoundland Faculty of Science
Jessica E. Besaw
Memorial University of Newfoundland Faculty of Science
Lisbeth Tranebjærg
University of Copenhagen Panum Institute: Kobenhavns Universitet Panum Instituttet
Nanna Dahl Rendtorff
University of Copenhagen Panum Institute: Kobenhavns Universitet Panum Instituttet
Kathy A. Hodgkinson
Memorial University of Newfoundland Faculty of Medicine
Leichelle A. Little
Western University
Sumit Agrawal
Western University
Lorne Parnes
Western University
Tony Batten
Memorial University of Newfoundland
Susan Moore
Memorial University of Newfoundland Faculty of Medicine
Pingzhao Hu
Memorial University of Newfoundland Faculty of Medicine

Justin A. Pater
Memorial University of Newfoundland Faculty of Medicine
Jim Houston
Memorial University of Newfoundland Faculty of Medicine
Dante Galutira
Memorial University of Newfoundland Faculty of Medicine
Tammy Benteau
Memorial University of Newfoundland Faculty of Medicine
Courtney MacDonald
Memorial University of Newfoundland Faculty of Medicine
Danielle French
Memorial University of Newfoundland Faculty of Medicine
Darren D. O'Rielly
Memorial University of Newfoundland Faculty of Medicine
Susan G. Stanton
Western University of Health Sciences
Terry-Lynn Young (tlyoung@mun.ca)
Memorial University of Newfoundland Faculty of Medicine https://orcid.org/0000-0003-4673-6470

Research Article

Keywords: FOXL1, clinical otosclerosis, autosomal dominant, OTSC, hearing loss

Posted Date: May 26th, 2021

DOI: https://doi.org/10.21203/rs.3.rs-539887/v1

Version of Record: A version of this preprint was published at Human Genetics on October 11th, 2021. See the published version at https://doi.org/10.1007/s00439-021-02381-1.

Abstract

Otosclerosis is a bone disorder of the otic capsule and common form of late-onset hearing impairment. Considered a complex disease, little is known about its pathogenesis. Over the past 20 years, ten autosomal dominant loci (*OTSC1-10*) have been mapped but no genes identified. Herein, we map a new *OTSC* locus to a 9.96 Mb region within the FOX gene cluster on 16q24.1 and identify a 15 bp coding deletion in Forkhead Box L1 co-segregating with otosclerosis in a Caucasian family. Phenotype ranges from moderate to severe hearing loss resolved by stapedectomy, to profound sensorineural loss requiring a cochlear implant. Mutant *FOXL1* is both transcribed and translated and correctly locates to the cell nucleus. However, the deletion of 5 residues in the C-terminus of mutant FOXL1 causes a complete loss of transcriptional activity due to loss of secondary (alpha helix) structure. *FOXL1* (rs764026385) was identified in a second unrelated case on a shared background. We conclude that *FOXL1* (rs764026385) is pathogenic and causes autosomal dominant otosclerosis and propose a key inhibitory role for wildtype Foxl1 in bone remodelling in the otic capsule. New insights into the molecular pathology of otosclerosis from this study provide molecular targets for non-invasive therapeutic interventions.

Introduction

Otosclerosis is a primary bone disorder of abnormal bone resorption and deposition in the otic capsule (bony labyrinth), and a common form of conductive hearing loss (HL). Although both environmental and genetic risk factors have been identified, pathogenesis of otosclerosis is unknown. Bone is a dynamic tissue that is continually remodelled, regulated by coupling signals between osteoclast and osteoblast cells involving interactions between a variety of factors including cytokines, chemokines, hormones and biochemical stimuli. Why skeletal bone remodelling is required for health is not fully understood; however, its imbalance leads to disease such as osteoporosis and inflammatory arthritis. The otic capsule is the rigid bony outer wall of the inner ear which protects the membranous labyrinth (endolymph-filled ducts) in its perilymph-filled cavities including the vestibule, semicircular canals and cochlea. It is also unique in that it undergoes little remodelling after maturation compared to skeletal bones (0.13 vs. 10% yearly) (Frisch et al. 2000). The otic capsule retains small remnants of embryonic tissue (globuli interossei) containing cartilage and quiescent osteoclast and osteoblasts. In early disease, it becomes highly vascularized with activated macrophages (osteoclast progenitors) causing foci of reabsorption of endochondral bone and deposition of new dense bone by osteoblasts (Babcock and Liu 2018). Invasion of these osteosclerotic foci into the stapediovestibular joint immobilizes the stapes resulting in conductive HL (Nager 1969). The key molecular triggers in the otic capsule activating remodelling and the onset of otosclerosis remain elusive (Babcock and Liu 2018).

Clinical otosclerosis has a preponderance for Caucasians of Northern European descent; first recognised as a common cause of HL in the 1800s (Ealy and Smith 2010), it is prevalent in 1/330 whites, 1/3300 blacks and 1/33,000 Asians (Thys and Van Camp 2009). Patients typically present with conductive HL which often progresses to mixed loss (cochlear otosclerosis); purely sensorineural hearing loss (SNHL) is rare. Onset is in the second, third or fourth decade and fortunately, the conductive component of otosclerosis is often successfully managed with a combination of stapes surgery and hearing aids (Cureoglu et al. 2006). In rare cases, a profound sensorineural deficit develops across all frequencies and requires cochlear implantation and electrical stimulation of the auditory nerve to restore hearing (Cureoglu et al. 2010). Histological otosclerosis refers to the observation that 4.5–12.5% of adult Caucasians show signs of otosclerosis post-mortem when temporal bones are examined. A definitive diagnosis of clinical otosclerosis requires visualization during surgery (Declau et al. 2001).

Although the majority of otosclerosis cases are considered sporadic, multiplex families have been used to map ten autosomal dominant (*OTSC*) loci to large genomic intervals: OTSC1 (Indian; 15q25-qter; 14.5Mb) (Tomek et al. 1998), OTSC2 (Belgian; 7q34-q36, 16Mb) (Van Den Bogaert et al. 2001), OTSC3 (Cypriot; 6p22.3-p21.3, 17.4Mb) (Chen et al.

2002), OTSC4 (Israeli; 16q22.1-q23.1, 10Mb) (Brownstein et al. 2006), OTSC5 (Dutch; 3q22-q24, 15.5 Mb) (Van Den Bogaert et al. 2004), OTSC6 (unpublished), OTSC7 (Greek; 6q13-q16.1, 13.47Mb) (Thys et al. 2007), OTSC8 (Tunisian; 9p13.1-q21.11, 34.16Mb) (Bel Hadj Ali et al. 2008), OTSC9 (unpublished) and OTSC10 (Dutch; 1q41-q44, 26.1Mb) (Schrauwen et al. 2011) between 1998 and 2010. Although individual risk contributions are small, case-control association studies have identified susceptibility variants in genes involved in bone remodelling [*COL1A* (McKenna et al. 1998; McKenna et al. 2004), *TGFB1* (Thys and Van Camp 2009), *BMP2* and *BMP4* (Schrauwen et al. 2008) and synaptic plasticity (*RELN*) (Schrauwen et al. 2009)]. Exploration of positional candidate genes in *OTSC2* patients suggests a potential role for the T-cell receptor-beta gene in the dysregulated development of T-cells (Schrauwen et al. 2010). More recently, rare variants in *SERPINF1* (Ziff et al. 2016) in familial otosclerosis showed promise but failed to validate in a larger case and family series (Valgaeren et al. 2019). Despite the 20 year lapse since the mapping of *OTSC1*, the *OTSC* genes remain refractory to discovery due to the rarity of monogenic families, diagnostic challenges and reduced penetrance. Herein, we map a new *OTSC* locus within the *FOX* gene cluster on 16q24.1 and identify *FOXL1* as the first *OTSC* gene.

Materials And Methods

Clinical Criteria and Evaluations

For linkage analyses (family-based study) we used conservative clinical criteria to assign affection status: affected were family members with otosclerosis confirmed by surgery; unaffected were blood relatives ≥ 60 years of age with normal (bilateral) hearing thresholds: all remaining members were considered "unknown status." All available medical charts and audiological reports were reviewed, and patients assessed, when possible, to update audiograms and confirm middle ear status. Classification of HL was based on the pure-tone threshold average of 0.5, 1.0 and 2.0 kHz as defined by the American Speech and Hearing Association (**Supplementary Information**).

Discovery Cohort

We have an ongoing recruitment drive for otosclerosis families from otolaryngology clinics in Newfoundland and Labrador (NL). One of the largest is Caucasian of English extraction segregating autosomal dominant otosclerosis of varied clinical presentation among seven surgically-confirmed cases (Table 1). Onset of HL ranges from mid-teens to early twenties. The proband at 25 years had bilateral conductive HL that progressed by age 51 to mixed asymmetric loss (R severe; L moderate-severe) with air-bone gaps averaging 50 dB and profound loss bilaterally at 8000 Hz (Fig. 1a, Table 1). Bilateral stapedectomies were clinically successful, with air-bone gaps resolved apart from slight residual conductive loss at 500 and 4000 Hz and functional hearing significantly restored at 52 years (Fig. 1a). High frequency thresholds show minimal improvement post-operatively, consistent with possible cochlear otosclerosis and/or presbycusis. The proband's parents (PIDs I-1, I-2, Fig. 2a) both have HL and several siblings (PID II-9, II-11, II-14) had a similar clinical course and successful post-stapedectomy resolution of conductive loss in one or both ears (Table 1). Although sibling PID II-2 had a similar early progression of conductive loss, stapedectomy (R) at age 36 was unsuccessful, resulting in profound loss with no response to stimuli. Amplification with a conventional hearing aid was used until no longer effective for severe mixed loss (L) (Table 1; Fig. 1a). PID II-2 had a middle ear implant at age 75 which was unsuccessful. Subsequent cochlear implantation at age 76 provided substantial functional improvement. Sibling PID II-3 had HL by mid-teens and wore hearing aids by age 18. No reliable responses to bone conduction stimuli were recorded on repeated tests from age 33–38, consistent with the medical report of profound SNHL bilaterally at age 38, and inadequate benefit from hearing aids (Fig. 1a; Table 1). At 60 years of age, CT imaging confirmed “prominent” otosclerosis in PID II-3. Stapedectomy (R) was attempted without success. Cochlear implantation at age 61 significantly improved hearing function (self-report). In the next generation, PID III-2 experienced an onset of conductive HL (R) in mid-teens, and was followed by surgical exploration at age 17, which identified stapes fixation and a cholesteatoma which

precluded stapedectomy. The report of a follow-up tympano-mastoidectomy to remove the cholesteatoma notes that the ossicular chain was left intact and re-mobilized; however, complete resolution of the air bone gap was not achieved (Fig. 1a, PID III-2, age 18) and subsequent ossicular re-mobilization achieved only temporary improvement. By age 35, the conductive loss had advanced to moderately severe (R) and moderate low frequency conductive loss (L) resulting in diagnosis of otosclerosis at age 35 (Fig. 1a).

Table 1
Hearing phenotypes pre- and post-stapedectomy in confirmed otosclerosis cases.

Subject (PID)	Onset (decade)	Hearing Loss Diagnosis (L = Left; R = Right)			Surgical Intervention/Clinical Outcome		
		Ear	Type	Degree	Procedure	Age in years	Functional Outcome
II-6 NL proband	3rd (early)	R	mixed	severe	stapedectomy	52	successful**
		L	mixed	moderately severe	stapedectomy	52	successful**
II-9	3rd (early)	R	conductive	severe	stapedectomy	47	partial success***
		L	conductive or mixed	unknown	stapedectomy	22	successful**
II-11	3rd (early)	R	sensorineural	mild-severe	none	-	-
		L	mixed	moderate-severe	stapedectomy	44	successful**
II-14	3rd (early)	R	conductive or mixed	Unknown	stapedectomy	37	successful**
		L	conductive or mixed	Unknown	stapedectomy	52	partial success***
II-2	3rd	R	conductive*	Severe*	stapedectomy	36	unsuccessful****
		L	mixed	Severe	middle ear implant	75	unsuccessful****
					cochlear implant	76	successful**
II-3	2nd	R	sensorineural	profound	stapedectomy	60	unsuccessful**** successful**
					cochlear Implant	61	
		L	sensorineural	profound	none	-	-
III-2	2nd	R	conductive*	unknown*	Tympanomastoidectomy (for cholesteatoma)	17	successful**
					& Stapes mobilization	17, 18	partial success***
		L	conductive	mild-moderate	none	-	-
IV-3 ON proband	3rd	R	mixed	profound	stapedectomy	62	successful**
		L	sensorineural	moderate low frequency	none	-	-

*based on physician's report

**near complete resolution of conductive loss post stapedectomy; significant improvement of functional hearing post implant

***hearing improved but significant conductive loss remains unresolved (> 20 dB air-bone gap at 2 or more frequencies)

Subject (PID)	Onset (decade)	Hearing Loss Diagnosis (L = Left; R = Right)			Surgical Intervention/Clinical Outcome		
		Ear	Type	Degree	Procedure	Age in years	Functional Outcome
****either no hearing improvement or deteriorated hearing post-operatively							

Validation Cohort

For validation purposes, we used unrelated otosclerosis cases recruited from Canada (n = 82), Finland (35) and Faroe Islands (n = 20). A positve hit was identified in an Ontario case with profound mixed loss (R) and moderate low frequency SNHL (L) (Fig. 1b, Table 1). Acoustic immittance testing revealed absent acoustic middle ear muscle reflexes despite normal middle ear compliance, a hallmark feature of otosclerosis. Hearing thresholds improved dramatically post-surgery, with near complete resolution of air-bone gaps, and noticeable improvement of bone conduction thresholds (Fig. 1b, age 67). Genealogical investigations yielded a multigenerational Caucasian family with autosomal dominant HL. This study was approved by institutional review boards at Memorial University (#1.186), Western University (#103679) and the Danish Research Ethical Committee (KF 01-234/02 and KF 01-108/03).

Linkage to Published *OTSC* Loci and Susceptibility Genes

Genomic DNA was isolated from peripheral leukocytes according to a standard salting out procedure.(Miller et al. 1988) Microsatellite markers were fluorescently labeled and amplified by PCR, run on ABI 3130xl or 3730 (Applied Biosystems) and analyzed with Gene Mapper v4.0. Pedigrees were drawn with Progeny (Progeny Genetics LLC) and haplotypes phased manually with the least number of recombination events. To test for linkage, seven family members (PID II-2, II-3, II-6, II-9, III-2, III-5, III-6; Fig. 2a) were genotyped for markers spanning each *OTSC* disease interval and bracketing three otosclerosis susceptibility genes (**Supplementary Information &** Table 1).

Sequencing, Variant Filtering and Validation

Positional candidate genes (UCSC Genome Browser and NCBI build 36.) were selected for sequencing based on function and/or gene expression. Samples were Sanger sequenced on an ABI 3130xl/3730. For first pass variant filtering, we used three affected (PID II-3, II-9, III-2) and an unaffected spouse (PID II-4) (Fig. 2a**)** and variants filtered (**Supplementary Information**).

Whole exome sequencing (WES) was performed to screen all positional candidate genes. We selected five affected (PIDs II-2, II-6, II-9, II-11, II-14) and two senior (55, 60 yrs old) population controls with normal hearing thresholds for first pass variant filtering (**Supplementary Information**). Variants of interest were validated by cascade sequencing. Heterozygous variants co-segregating with otosclerosis in an autosomal dominant pattern were tested in unrelated otosclerosis cases. Positive hits were genotyped and examined for potential allele sharing with the disease haplotype identified in the NL family.

Computer Modelling of 2D Structure of Mutant Foxl1 C-Terminus

To assess the effect of the missing residues on FOXL1 structure, simulations were performed with the NAMD software (version 2.12) (Khajeh et al. 2020). The structure of the most C-terminal 69 residues of wildtype ($FOXL1_{CTERM}$) and the deletion mutant ($FOXL1_{MUT}$) were deduced by molecular dynamics simulations. Initial structures were generated in an extended state using the Protein in Atomistic details coupled with Coarse-grained Environment (PACE) model (Han and

Schulten 2012). Replica exchange molecular dynamics (REMD) (Zhou 2007) was then employed to sample the folded configurational space of these proteins (**Supplementary Information**).

Experimental Measurements of 3D Structure of Mutant Foxl1 C-Terminus

To validate modelling of the 3D structure, $FOXL1_{MUT}$ and $FOXL1_{CTERM}$ were produced recombinantly in *E. coli*, purified by nickel affinity chromatography followed by size exclusion chromatography. Circular dichroism measurements were carried out on a Jasco J-810 spectropolarimeter (Jasco Inc.) in the far ultraviolet range (190–260 nm) with a 0.5 mm quartz cuvette at RT (average of 20 scans).

Cell Culture and RNA Extractions

RNA was extracted from transformed B-cell lymphocytes from both affected and unaffected individuals (controls) using TRIzol-based methods (Thermo-fisher, Cat. #15596026). Osteoblast (hFOB 1.19) and HEK293A cell lines (ATCC) were maintained as adherent cells in Iscove's Modified Dulbecco's Medium (IMDM) F/12 (Life Technologies) maintained and total RNA extracted (**Supplementary Information**).

FOXL1 Expression Constructs

To investigate the effect of the *FOXL1* 15-bp deletion on function, we transfected osteoblast cell line (hFOB1.19) with *FOXL1-WT* and *FOXL1-MUT* expression plasmids. We purchased two expression vector constructs from GeneCopoeia containing wild type *FOXL1* (NM_005250) and generated two mutant constructs (*FOXL1* c.976_990del) by site directed mutagenesis (NOROCLONE biotech laboratories), using two empty plasmids as mock controls (**Supplementary Information**).

Western Blot

To determine the effect of the *FOXL1* deletion on the quantity and location of Foxl1 protein, we used osteoblast cells transfected with the wildtype and mutant constructs and immunoblotting. *FOXL1* expression was determined using Anti-FOXL1 rabbit polyclonal IgG (ab83000, Abcam) (1µg/ml). Housekeeping proteins were detected with α tubulin (clone DM1A + DM1B, Abcam) (200 µg/ml) and anti-nuclear matrix protein p84 antibody (clone 5E10, Abcam) (1µg/ml) (**Supplementary Information**). Immunoreactivity was visualized by scanning densitometry (Image Quant LAS 4000) and quantified (Image GE software) (GE Healthcare).

Fluorescence Microscopy

Transfected HFOB1.19 cells were visualized with a Carl Zeiss AxioObserver A.1 microscope with standard fluorescence and brightfield/darkfield settings at X5 0,25 or X20 0,50 NA objectives. Images were captured using a Zeiss AxioCam MRM3 camera with Zeiss AxioVision 4.8 software. GFP-transfected cells were harvested by trypsin, followed by fixation in 1.0% paraformaldehyde (Sigma), and analysis of 5000–10,000 cells using a FACS Calibur flow cytometer (Becton-Dickinson).

Luciferase Reporter Assay

To determine if the removal of 5 C-terminus residues in FOXL1 alters its ability to activate downstream transcription, we used a luciferase reporter assay. The reporter construct contained two copies of the *FOXL1* Consensus binding sequence [TATACATAAACAAGAA] (Pierrou et al. 1994) cloned into pGL3 (Promega) upstream of the *thymidine kinase* minimal promoter and the luciferase open reading frame (*Photinus*) (**Supplementary Information**). Ratios of *Photinus* and *Renilla* luciferase were calculated, and wildtype and mutant readings were compared to those from the empty expression vector

(which was standardized to 1). Data are graphed as mean fold change +/- SD. A Fluoroskan Ascent (Labsystems) was used for all readings.

Results

Otosclerosis is Not Linked to Published *OTSC* Loci or Susceptibility Genes

In the NL family, recapitulating haplotypes mapping to published *OTSC* loci [*OTSC1* (15q25-q26), *OTSC2* (7q34q36), *OTSC3* (6p21.3-p22.3), *OTSC4* (16q22.1-q23.1), *OTSC5* (3q22-24), *OTSC7* (6q13-16.1), *OTSC8* (9p13.1-9q2*)*, *OTSC10* (1q41-q44)] and susceptibility genes [*COL1A1*, *COL1A2*, *NOG*] failed to identify shared haplotypes among surgically confirmed cases (Abdelfatah 2014). Furthermore, significantly negative two-point LOD scores (< 2.0) supported linkage exclusion across all published *OTSC* loci (**Supplementary Table 2**). The proband also screened negative for rare variants recently identified in the *SERPINF1* gene (Ziff et al. 2016).

New *OTSC* Locus Maps to 16q24

Serendipitously, we noted allele sharing among affected members of the NL family for markers near the *OTSC4* qter boundary (Brownstein et al. 2006). Increased recruiting efforts and extensive genotyping on all available relatives mapped a disease-associated haplotype 12 Mb downstream of *OTSC4*. Using both affected and unaffected members, we identified key recombination events to the disease haplotype and defined a new *OTSC* locus spanning 9.96 Mb on 16q24 (Fig. 2a). Furthermore, two-point linkage analysis of the 16q24 markers yielded positive LOD scores (> 1.5) suggestive of linkage (**Supplementary Table 2**).

Rare Coding In-Frame Deletion in *FOXL1* identified

Using the discovery cohort, Sanger sequencing of 12 positional candidates (*PLCG2, IRF8, SCL38A8, ZDHHC7, SLC7A5, HSD17B2, COTL1, FOXF1, FOXL1, FOXC1, CA5A*, *OSGIN*) spanning the new *OTSC* locus on 16q24 yielded 92 variants. Of these, 91 variants were filtered out because they were either absent in affected samples, present in the unaffected spouse, had a MAF > 2% or predicted *in silico* tools to be benign. We identified a novel variant, an in-frame deletion of 15bps in the transcription factor *FOXL1* (NM_005250.3: c.976_990del), that was both absent in 116 ethnically matched controls and co-segregated with otosclerosis in the NL family (Fig. 2a, b). Subsequently, WES of all positional candidate genes uncovered two additional variants (*PKD1L2*; c.749 A > G and c.658 C > T); however, these variants subsequently failed segregation analysis. No other SNPs/deletions were detected. *FOXL1* has a single exon encoding a 345 aa transcription factor and resides in a gene cluster on 16q24.1 with *FOXC2* and *FOXF1*. The 15bp in-frame deletion predicted the removal of residues 326–330 (GIPFL) from the C terminus of *Foxl1* (Fig. 2c). The *FOXL1* (rs764026385) variant has been subsequently reported to have a global frequency of 0.211% [highest in European (non-Finnish) subpopulation at 0.247%; rarest in the African subpopulation at 0.060%; gnomAD] but has not been reported in Clinvar or ClinGen. A single report in Varsome classified this variant as a VUS according to ACMG criteria.(Richards et al. 2015a) Targeted screening of *FOXL1* (rs764026385) in the unrelated otosclerosis series identified a Canadian case (PID IV-3, Fig. 2d) from the province of Ontario with allele sharing, suggesting a common ancestor (Fig. 2e).

Structural Consequences of Deletion *FOXL1* p.(Gly326_Leu330del)

The in-frame deletion of five residues in the C-terminal domain of *FOXL1* in otosclerosis patients occurs in the most ordered and evolutionary-conserved portion of FOXL1. Simulations showed that removal of residues GIPFL disrupted the hydrophobic core resulting in an increasing randomly coiled structure (Fig. 3a). The C-terminus of the wildtype and mutant FOXL1 were also produced recombinantly in *E. coli* and their secondary structure probed experimentally by circular dichroism (CD). As indicated by the difference in ellipticity at 222 nm, the wildtype structure has twice as much

helix as the mutant, suggesting that the mutant and wild type proteins have substantially different structures, the mutant being more random coil, while the wild type has a substantial amount of alpha helix (Fig. 3a). We estimate that C-terminus of the mutant FOXL1 has 48% of the helicity of wildtype FOXL1.

Functional Consequences of *FOXL1* p.(Gly326_Leu330del)

As *FOXL1* RNA expression level was undetectable using transformed B-cell lymphocytes from subjects, cell lines were transfected with either FOXL1-^{WT} or FOXL1-^{MUT} expression plasmids to compare gene and protein expression. Osteoblast cell lines (hFOB1.19) transfected with either FOXL1-^{WT} or FOXL1-^{MUT} expression plasmids show a high level of RNA expression with RT-PCR Taqman assay (Fig. 3b). Transfection efficiency was identical in both wild type and mutant *FOXL1* constructs. Immunoblotting revealed FOXL1 protein was significantly increased (**$p < 0.01$) in the mutant and expression was localized to the nucleus (Fig. 3c). Expression of wildtype and mutant FOXL1:GFP fusion proteins in HEK293 cells also indicates that wildtype FOXL1 localizes to the nucleus (Fig. 3d). To test the transcriptional activity of mutant *FOXL1*, using human HEK293 cells, we constructed a luciferase reporter with two copies of the *FOXL1* consensus binding sequence to drive expression from a minimal promoter (thymidine kinase). While transient transfection of the wildtype *FOXL1* constructs increased luciferase expression 42% over endogenous levels, no transcriptional activity ($p = 7x10^{-9}$) above endogenous levels was observed in cells transfected with the *FOXL1* mutant (Fig. 3e). Taken together, we conclude that *FOXL1* (NM_005250.2: c.976_990del) is pathogenic according to conservative criteria (PS3, PM2, PM4, PP1, PP3, PP4) (Richards et al. 2015b) and the cause of autosomal dominant otosclerosis in this study.

Discussion

We have mapped and identified the first *OTSC* gene, Forkhead Box L1, in a Caucasian family of English extraction. Using haplotype and linkage exclusion, we ruled out previously published *OTSC* loci and several associated genes and mapped a new *OTSC* locus within the FOX gene cluster on chromosome 16q24.1. Significant research resources were dedicated to family recruitment and clinical assessment, which turned out to be essential to mapping the new *OTSC* locus and identifying the causal gene by reducing the number of rare heterozygous variants that required functional follow-up. RNA and protein investigations reveal that *FOXL1* deletion variant is both transcribed and translated and correctly localizes to the cell nucleus. However, the missing residues in the C terminus of mutant FOXL1 causes significant loss of helical structure, rendering the mutant transcription factor devoid of transcriptional activity suggesting haploinsufficiency. A second unrelated Caucasian case was heterozygous for *FOXL1* (rs764026385) and resides on the same disease haplotype as the NL family, suggesting a common ancestor and the likelihood that this *OTSC* gene was imported to North America from Northern Europe.

Clinical otosclerosis due to *FOXL1* spans the full phenotypic range characteristic of otosclerosis, from substantial conductive HL resolved by surgery to profound sensorineural loss requiring cochlear implantation. While surgical intervention has been a viable and beneficial treatment to improve hearing for many cases, we see from the NL family that success is not guaranteed and not all forms of otosclerosis are amenable to surgical therapy. Furthermore, individuals with severe cochlear otosclerosis may be fitted with conventional hearing aids for years with minimal benefit.

In skeletal bones, bone remodelling is determined by the interplay between receptor activator of nuclear factor (NF)-kB-ligand (RANKL), which binds to the receptor activator of NF-kB (RANK) on progenitors inducing osteclastogenesis and osteoprotegerin (OPG), which prevents RANKL from binding to RANK. In the otic capsule, the same RANK, RANKL and OPG axis is at play, however bone turnover is suppressed by the release of OPG into the perilymph by fibrocytes in the spiral ligament (cochlear lateral wall). High levels of OPG maintain this suppression in the membranous labyrinth of the inner ear. OPG binding to RANKL regulate both bone resorption and spiral ganglion degeneration, as studies in knockout

Opg − /− mice reveal the development of conductive hearing pathology due to abnormal bone growth and SNHL caused by auditory nerve degeneration (Kao et al. 2013).

FOX proteins are a super family of transcription factors that play increasingly recognised roles in a diverse range of developmental processes such as the establishment of the body axis and the development of tissues from all three germ layers. Specifically, FOX proteins lie at the junction of multiple signalling pathways and play crucial roles in regulating gene expression in cell metabolism, proliferation, differentiation and apoptosis (Lam et al. 2013). In the last decade, the identification of causal genes for rare, monogenic skeletal dysplasia have provided novel insights into the role and functioning of the Wingless and int-1 (WNT) signalling pathway. The result of discoveries in monogenic dysplasia, the WNT signalling pathway is known to be important in both skeletal development and bone homeostasis. In the otic capsule, *FOXL1* likely acts upon the globuli interossei containing cartilage and quiescent osteoclast and osteoblasts. Zebrafish studies show that *Foxl1* can have both transcriptional activation and repression functions and transcriptional repressor Foxl1 regulates central nervous system development by suppressing sonic hedgehog (shh) expression (Nakada et al. 2006).

In the NL family, PID III-2 was diagnosed with cholesteatoma at 17 years of age. β-catenin (part of WNT pathway) expression is increased in cholesteatoma cells when compared with normal epithelium cells and we postulate that cholesteatoma, like otosclerosis, may be a result of mutation in *FOXL1*, given reported cases of familial cholesteatoma, including rare autosomal dominant families (Collins et al. 2020; Jennings et al. 2018). Industry focus on pharmacologically modulating the Wnt signalling pathway in cancer provides a potential treatment option for otosclerosis and possibly cholesteatoma as well (Zimmerli et al. 2017).

Strengths of this study included conservative "affected" status that avoided phenocopies, particularly important with phenotypes like HL that are common, as we see in the NL family with HL on both the maternal and paternal sides of the pedigree. It is also important to recognise that phenotypes change over time, and multiple distinct diagnosis may represent the changing face of a monogenetic disorder under study in a large family. Discerning otosclerosis from other HL aetiologies was critical to this successful gene hunt as variant filtering with just one incorrect affected or unaffected case would derail gene discovery. A comprehensive approach using traditional (linkage and haplotype analysis) in combination with new (NGS) technologies and significant resources to recruit and clinically assess blood relatives helped minimize the critical disease interval to the smallest among published *OTSC* loci. Heterozygous *FOXL1* subjects (PID III-1 & PID-III-6) will be important to follow to determine if they are pre-clinical or non-penetrant.

Limitations of this study include a limited series of otosclerosis cases which precluded our ability to estimate the percentage of *FOXL1* cases in Northern Europeans. The *FOXL1* deletion is most frequent in Europe and rarest in Africa, which may contribute to the low prevalence of otosclerosis in Africa. A much larger, global case series is required to evaluate the contribution of *FOXL1* to both Mendelian and sporadic otosclerosis cases. Uncorrectable ascertainment, where the most clinically affected families are recruited, is an essential design feature of gene hunts, but will likely overestimate the true penetrance of any gene. In addition, time to forge collaborations to successfully complete multiple functional studies added to the time from gene discovery to publication, a recognised challenge to the timely publication of new gene discoveries (Bamshad et al. 2019).

We call for renewed efforts to identify all *OTSC* genes, as determining the factors that trigger bone turnover in the inner ear remain elusive. The combination of positional cloning and NGS was successful in this study and so far has resolved 92 % of the monogenic skeletal dysplasias (Huybrechts et al. 2020). Otosclerosis is considered to be 40% penetrant (Moumoulidis et al. 2007); however, the true penetrance of each *OTSC* mutation awaits their discovery and testing to identify gene carriers in the general population in order to circumvent ascertainment bias. Although developing animal models of *OTSC* genes will provide mechanistic insights into disease pathology, accurate diagnosis and therapeutic

treatment of otosclerosis requires the identification of all the *OTSC* genes. As stated by Bamshad *et al*. "*the vast majority of variants of known function in the human genome underlie Mendelian conditions, and the study of natural genome variation manifest by Mendelian conditions still provides a time-efficient and cost-effective path to link genotype with human phenotype*" (Bamshad et al. 2019). This study provides new insights into genes and pathways involved in osteosclerosis and renewed hope for therapeutic options for otosclerosis and perhaps other disorders are now within striking distance.

Web Resources

Amer Speech &Hearing Assoc, https://www.asha.org/practice-portal/clinical-topics/hearing-loss/

ATTC, https://www.atcc.org/

Burrows-Wheeler Aligner BWA, http://bio-bwa.sourceforge.net/

ClinGen, https://clinicalgenome.org/

ClinVar, https://www.ncbi.nlm.nih.gov/clinvar/

ClustalW, https://www.genome.jp/tools-bin/clustalw

dbSNP, https://www.ncbi.nlm.nih.gov/snp/

gnomAD, https://gnomad.broadinstitute.org/

Hereditary Hearing Loss homepage, http://hereditaryhearingloss.org/

Human Splicing Finder, www.umd.be/HSF3/

NCBI, ncbi.nlm.nih.gov/

OMIM, https://www.ncbi.nlm.nih.gov/omim

1000 genomes, https://www.internationalgenome.org/home

Primer3, https://bioinfo.ut.ee/primer3-0.4.0/

PANTHER, http://www.pantherdb.org/

PolyPhen-2, http://genetics.bwh.harvard.edu/pph2/

RefSeq, https://www.ncbi.nlm.nih.gov/refseq/

SIFT, https://sift.bii.a-star.edu.sg/

SNP database, http://www.ncbi.nlm.nih.gov/projects/SNP/

Varsome, http://varsome.com

Weblogo, https://weblogo.berkeley.edu/logo.cgi

UCSC Genome Browser, https://genome.ucsc.edu/

Declarations

Acknowledgements

We are grateful to the study participants and to Elspeth Drinkell and Carol Negrijn for drawing pedigrees. This study was funded by the Canadian Institutes of Health Research (#222294), Canadian Foundation for Innovation (#9384, #13120), and Genome Canada/Genome Atlantic (AMGGI). Support was also provided by the Janeway Children's Hospital Foundation, Memorial University, Town of Grand Falls-Windsor (Excite Corporation) and the Government of Newfoundland and Labrador. The first author N.A. is a Canadian Institutes of Health Research-Fellowship awardee.

Availability of data and material

The datasets generated during and/or analysed during the current study are available from the corresponding author on reasonable request.

Code availability

Not Applicable

Authors' contributions

Study design: N.A, S.G.S, T.L.Y. Clinical studies: S.G.S, A.G., M.B.L., S.S., N.A., L.A.L., K.A.H, A.B., S.A., L.P.; Molecular studies: N.A., D.G., J.H., T.B., C.P., M.B.L. Functional studies: A.M., C.R.F., J.A.P., D.F, C.M. Structural studies. V.B., C.R., J.E.B. Statistics/Bioinformatic Analysis: P.H., D.D.O. European data contributed by L.T. and N.D.R. Manuscript Writing: N.A., D.D.O and T.L.Y.

Conflicts of Interests

The authors declare they have no conflict of interest.

Ethics Approval

This study was approved by institutional review boards at Memorial University (#1.186), Western University (#103679) and the Danish Research Ethical Committee (KF 01-234/02 and KF 01-108/03).

Consent to participate

Informed consent was obtained from all individual participants included in the study.

Consent for Publication

Participants signed informed consent regarding publishing their data.

References

Abdelfatah N (2014) The genetic aetiology of otosclerosis in the population of Newfoundland and Labrador. Doctoral dissertation. .Memorial University of Newfoundland, Canada.

Babcock TA, Liu XZ (2018) Otosclerosis: From Genetics to Molecular Biology. Otolaryngol Clin North Am 51: 305-318. doi: 10.1016/j.otc.2017.11.002

Bamshad MJ, Nickerson DA, Chong JX (2019) Mendelian Gene Discovery: Fast and Furious with No End in Sight. Am J Hum Genet 105: 448-455. doi: 10.1016/j.ajhg.2019.07.011

Bel Hadj Ali I, Thys M, Beltaief N, Schrauwen I, Hilgert N, Vanderstraeten K, Dieltjens N, Mnif E, Hachicha S, Besbes G, Ben Arab S, Van Camp G (2008) A new locus for otosclerosis, OTSC8, maps to the pericentromeric region of chromosome 9. Hum Genet 123: 267-72. doi: 10.1007/s00439-008-0470-3

Brownstein Z, Goldfarb A, Levi H, Frydman M, Avraham KB (2006) Chromosomal mapping and phenotypic characterization of hereditary otosclerosis linked to the OTSC4 locus. Arch Otolaryngol Head Neck Surg 132: 416-24. doi: 10.1001/archotol.132.4.416

Chen W, Campbell CA, Green GE, Van Den Bogaert K, Komodikis C, Manolidis LS, Aconomou E, Kyamides Y, Christodoulou K, Faghel C, Giguére CM, Alford RL, Manolidis S, Van Camp G, Smith RJ (2002) Linkage of otosclerosis to a third locus (OTSC3) on human chromosome 6p21.3-22.3. J Med Genet 39: 473-7. doi: 10.1136/jmg.39.7.473

Collins R, Ta NH, Jennings BA, Prinsley P, Philpott CM, Steel N, Clark A (2020) Cholesteatoma and family history: An international survey. Clin Otolaryngol 45: 500-505. doi: 10.1111/coa.13544

Cureoglu S, Baylan MY, Paparella MM (2010) Cochlear otosclerosis. Curr Opin Otolaryngol Head Neck Surg 18: 357-62. doi: 10.1097/MOO.0b013e32833d11d9

Cureoglu S, Schachern PA, Ferlito A, Rinaldo A, Tsuprun V, Paparella MM (2006) Otosclerosis: etiopathogenesis and histopathology. Am J Otolaryngol 27: 334-40. doi: 10.1016/j.amjoto.2005.11.001

Declau F, Van Spaendonck M, Timmermans JP, Michaels L, Liang J, Qiu JP, Van de Heyning P (2001) Prevalence of otosclerosis in an unselected series of temporal bones. Otol Neurotol 22: 596-602. doi: 10.1097/00129492-200109000-00006

Ealy M, Smith RJ (2010) The genetics of otosclerosis. Hear Res 266: 70-4. doi: 10.1016/j.heares.2009.07.002

Frisch T, Sorensen MS, Overgaard S, Bretlau P (2000) Estimation of volume referent bone turnover in the otic capsule after sequential point labeling. Ann Otol Rhinol Laryngol 109: 33-9. doi: 10.1177/000348940010900106

Han W, Schulten K (2012) Further optimization of a hybrid united-atom and coarse-grained force field for folding simulations: Improved backbone hydration and interactions between charged side chains. Journal of chemical theory and computation 8: 4413-4424. doi: 10.1021/ct300696c

Huybrechts Y, Mortier G, Boudin E, Van Hul W (2020) WNT Signaling and Bone: Lessons From Skeletal Dysplasias and Disorders. Front Endocrinol (Lausanne) 11: 165. doi: 10.3389/fendo.2020.00165

Jennings BA, Prinsley P, Philpott C, Willis G, Bhutta MF (2018) The genetics of cholesteatoma. A systematic review using narrative synthesis. Clin Otolaryngol 43: 55-67. doi: 10.1111/coa.12900

Kao SY, Kempfle JS, Jensen JB, Perez-Fernandez D, Lysaght AC, Edge AS, Stankovic KM (2013) Loss of osteoprotegerin expression in the inner ear causes degeneration of the cochlear nerve and sensorineural hearing loss. Neurobiol Dis 56: 25-33. doi: 10.1016/j.nbd.2013.04.008

Khajeh K, Aminfar H, Masuda Y, Mohammadpourfard M (2020) Implementation of magnetic field force in molecular dynamics algorithm: NAMD source code version 2.12. J Mol Model 26: 106. doi: 10.1007/s00894-020-4349-0

Lam EW, Brosens JJ, Gomes AR, Koo CY (2013) Forkhead box proteins: tuning forks for transcriptional harmony. Nat Rev Cancer 13: 482-95. doi: 10.1038/nrc3539

McKenna MJ, Kristiansen AG, Bartley ML, Rogus JJ, Haines JL (1998) Association of COL1A1 and otosclerosis: evidence for a shared genetic etiology with mild osteogenesis imperfecta. Am J Otol 19: 604-10.

McKenna MJ, Nguyen-Huynh AT, Kristiansen AG (2004) Association of otosclerosis with Sp1 binding site polymorphism in COL1A1 gene: evidence for a shared genetic etiology with osteoporosis. Otol Neurotol 25: 447-50. doi: 10.1097/00129492-200407000-00008

Miller SA, Dykes DD, Polesky HF (1988) A simple salting out procedure for extracting DNA from human nucleated cells. Nucleic Acids Res 16: 1215. doi: 10.1093/nar/16.3.1215

Moumoulidis I, Axon P, Baguley D, Reid E (2007) A review on the genetics of otosclerosis. Clin Otolaryngol 32: 239-47. doi: 10.1111/j.1365-2273.2007.01475.x

Nager GT (1969) Histopathology of otosclerosis. Arch Otolaryngol 89: 341-63. doi: 10.1001/archotol.1969.00770020343022

Nakada C, Satoh S, Tabata Y, Arai K, Watanabe S (2006) Transcriptional repressor foxl1 regulates central nervous system development by suppressing shh expression in zebra fish. Mol Cell Biol 26: 7246-57. doi: 10.1128/MCB.00429-06

Pierrou S, Hellqvist M, Samuelsson L, Enerbäck S, Carlsson P (1994) Cloning and characterization of seven human forkhead proteins: binding site specificity and DNA bending. Embo j 13: 5002-12.

Richards S, Aziz N, Bale S, Bick D, Das S, Gastier-Foster J, Grody WW, Hegde M, Lyon E, Spector E, Voelkerding K, Rehm HL (2015a) Standards and guidelines for the interpretation of sequence variants: a joint consensus recommendation of the American College of Medical Genetics and Genomics and the Association for Molecular Pathology. Genet Med 17: 405-24. doi: 10.1038/gim.2015.30

Richards S, Aziz N, Bale S, Bick D, Das S, Gastier-Foster J, Grody WW, Hegde M, Lyon E, Spector E, Voelkerding K, Rehm HL, Committee ALQA (2015b) Standards and guidelines for the interpretation of sequence variants: a joint consensus recommendation of the American College of Medical Genetics and Genomics and the Association for Molecular Pathology. Genetics in medicine : official journal of the American College of Medical Genetics 17: 405-424. doi: 10.1038/gim.2015.30

Schrauwen I, Ealy M, Huentelman MJ, Thys M, Homer N, Vanderstraeten K, Fransen E, Corneveaux JJ, Craig DW, Claustres M, Cremers CW, Dhooge I, Van de Heyning P, Vincent R, Offeciers E, Smith RJ, Van Camp G (2009) A genome-wide analysis identifies genetic variants in the RELN gene associated with otosclerosis. Am J Hum Genet 84: 328-38. doi: 10.1016/j.ajhg.2009.01.023

Schrauwen I, Thys M, Vanderstraeten K, Fransen E, Dieltjens N, Huyghe JR, Ealy M, Claustres M, Cremers CR, Dhooge I, Declau F, Van de Heyning P, Vincent R, Somers T, Offeciers E, Smith RJ, Van Camp G (2008) Association of bone morphogenetic proteins with otosclerosis. J Bone Miner Res 23: 507-16. doi: 10.1359/jbmr.071112

Schrauwen I, Venken K, Vanderstraeten K, Thys M, Hendrickx JJ, Fransen E, Van Laer L, Govaerts PJ, Verstreken M, Schatteman I, Stinissen P, Hellings N, Van Camp G (2010) Involvement of T-cell receptor-beta alterations in the development of otosclerosis linked to OTSC2. Genes Immun 11: 246-53. doi: 10.1038/gene.2010.3

Schrauwen I, Weegerink NJ, Fransen E, Claes C, Pennings RJ, Cremers CW, Huygen PL, Kunst HP, Van Camp G (2011) A new locus for otosclerosis, OTSC10, maps to chromosome 1q41-44. Clin Genet 79: 495-7. doi: 10.1111/j.1399-0004.2010.01576.x

Thys M, Van Camp G (2009) Genetics of otosclerosis. Otol Neurotol 30: 1021-32. doi: 10.1097/MAO.0b013e3181a86509

Thys M, Van Den Bogaert K, Iliadou V, Vanderstraeten K, Dieltjens N, Schrauwen I, Chen W, Eleftheriades N, Grigoriadou M, Pauw RJ, Cremers CR, Smith RJ, Petersen MB, Van Camp G (2007) A seventh locus for otosclerosis, OTSC7, maps to chromosome 6q13-16.1. Eur J Hum Genet 15: 362-8. doi: 10.1038/sj.ejhg.5201761

Tomek MS, Brown MR, Mani SR, Ramesh A, Srisailapathy CR, Coucke P, Zbar RI, Bell AM, McGuirt WT, Fukushima K, Willems PJ, Van Camp G, Smith RJ (1998) Localization of a gene for otosclerosis to chromosome 15q25-q26. Hum Mol Genet 7: 285-90. doi: 10.1093/hmg/7.2.285

Valgaeren H, Sommen M, Beyens M, Vandeweyer G, Schrauwen I, Schepers A, Schatteman I, Topsakal V, Dhooge I, Kunst H, Zanetti D, Huber AM, Hoischen A, Fransen E, Van Camp G (2019) Insufficient evidence for a role of SERPINF1 in otosclerosis. Mol Genet Genomics 294: 1001-1006. doi: 10.1007/s00438-019-01558-8

Van Den Bogaert K, De Leenheer EM, Chen W, Lee Y, Nurnberg P, Pennings RJ, Vanderstraeten K, Thys M, Cremers CW, Smith RJ, Van Camp G (2004) A fifth locus for otosclerosis, OTSC5, maps to chromosome 3q22-24. J Med Genet 41: 450-3. doi: 10.1136/jmg.2004.018671

Van Den Bogaert K, Govaerts PJ, Schatteman I, Brown MR, Caethoven G, Offeciers FE, Somers T, Declau F, Coucke P, Van de Heyning P, Smith RJ, Van Camp G (2001) A second gene for otosclerosis, OTSC2, maps to chromosome 7q34-36. Am J Hum Genet 68: 495-500. doi: 10.1086/318185

Zhou R (2007) Replica exchange molecular dynamics method for protein folding simulation. In: Bai Y (ed) Protein Folding Protocols. Methods in Molecular Biology, vol 350. Humana Press)

Ziff JL, Crompton M, Powell HR, Lavy JA, Aldren CP, Steel KP, Saeed SR, Dawson SJ (2016) Mutations and altered expression of SERPINF1 in patients with familial otosclerosis. Hum Mol Genet 25: 2393-2403. doi: 10.1093/hmg/ddw106

Zimmerli D, Hausmann G, Cantu C, Basler K (2017) Pharmacological interventions in the Wnt pathway: inhibition of Wnt secretion versus disrupting the protein-protein interfaces of nuclear factors. Br J Pharmacol 174: 4600-4610. doi: 10.1111/bph.13864

Figures

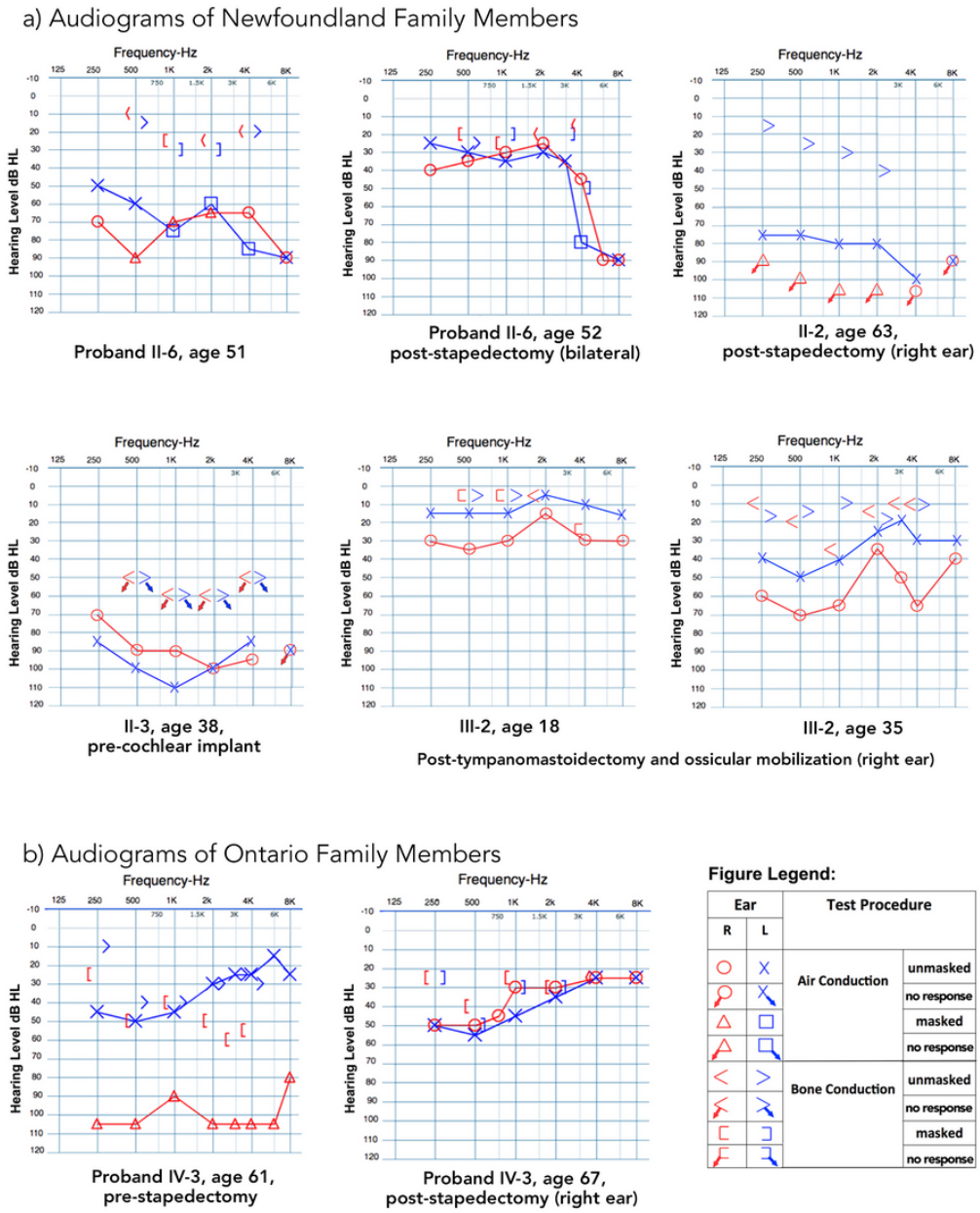

Figure 1

Selected Audiograms of Otosclerosis Cases Pre- and Post-Stapedectomy. (a) The NL proband (PID II-6) at age 51 showing extensive bilateral air-bone gaps, largely resolved by age 52 after bilateral stapedectomies. PID II-2 at age 63 presents with no measurable hearing after unsuccessful stapedectomy (R), and severe mixed loss (L). PID II-3 at age 38 presents with profound HL and no measurable bone conduction thresholds (bilateral). PID III-2 at age 18 shows normal hearing (L) and residual conductive loss following tympano-mastoidectomy and stapes re-mobilization (R), however subsequent re-mobilization of right ear ossicles is not sustained and by age 35, conductive HL has progressed bilaterally. (b) The Ontario case at age 63 shows profound mixed HL (R) and moderate low frequency sensorineural loss (L). By age 67 and following stapedectomy (R), air-bone gaps are largely resolved, and some bone conduction thresholds are improved (R) and bilateral HL is essentially symmetrical.

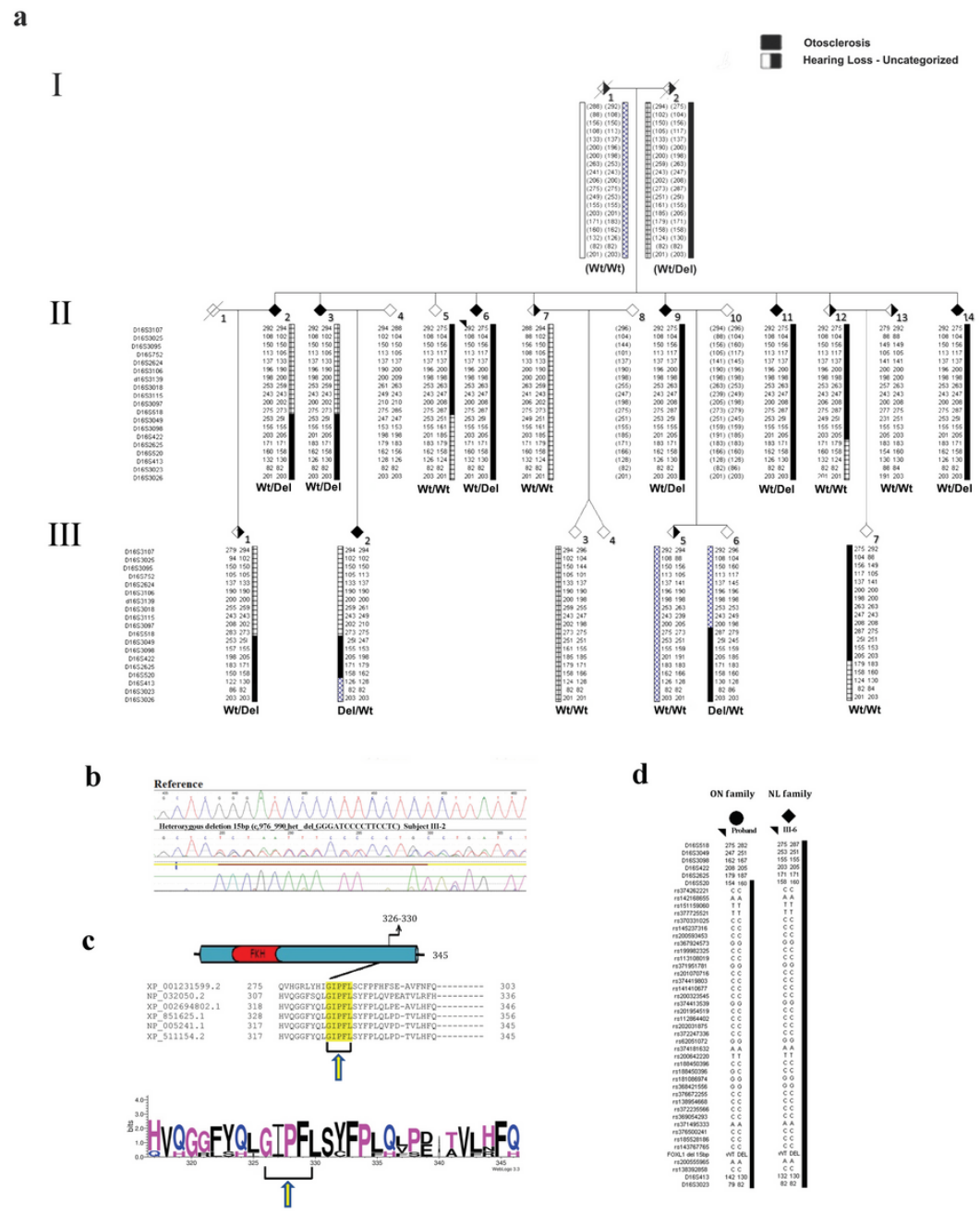

Figure 2

Co-segregation of a 15bp In-Frame Deletion in Forkhead Box L1 (FOXL1, rs764026385) with Otosclerosis and Alignment of Orthologs. (a) The family from Newfoundland and Labrador (NL) with 7 confirmed otosclerosis cases (filled symbols) used to map a new OTSC locus within the FOX gene cluster on chromosome 16q24.1. Recombination events to the disease haplotype (black) in siblings PIDs II-2, II-3 and II-5 positioned the causal gene qter of marker D16S518; a recombination in PID III-2 positioned the causal gene pter of D16S413. Taken together, these events refined the disease interval to a 9.96 Mb region on 16q24. Mutation status [Wt=wildtype; Del= FOXL1(rs764026385)] is shown and sex is masked (diamond symbol) to protect privacy. (b). Electropherogram of subject PID III-2 heterozygous for FOXL1 (rs764026385). (c) Schematic of mutant Foxl1 (FKH=Fork head domain) with Weblogo display of aa conservation and the five missing residues (yellow) in the C-terminus of Foxl1; species [G.allus; XP_001231599.2, M.musculus; NP_032050.2, B.taurus;XP_002694802.1, C.lupus; XP_851625.1, Homo sapiens; NP_005241.1, p.troglodytes; XP_511154.2]. (d) Comparison of disease haplotype (black) within the critical disease interval (D16S520-D16S413)

reveals haplotype sharing between the NL proband and the Ontario case, both are heterozygous for FOXL1 (rs764026385).

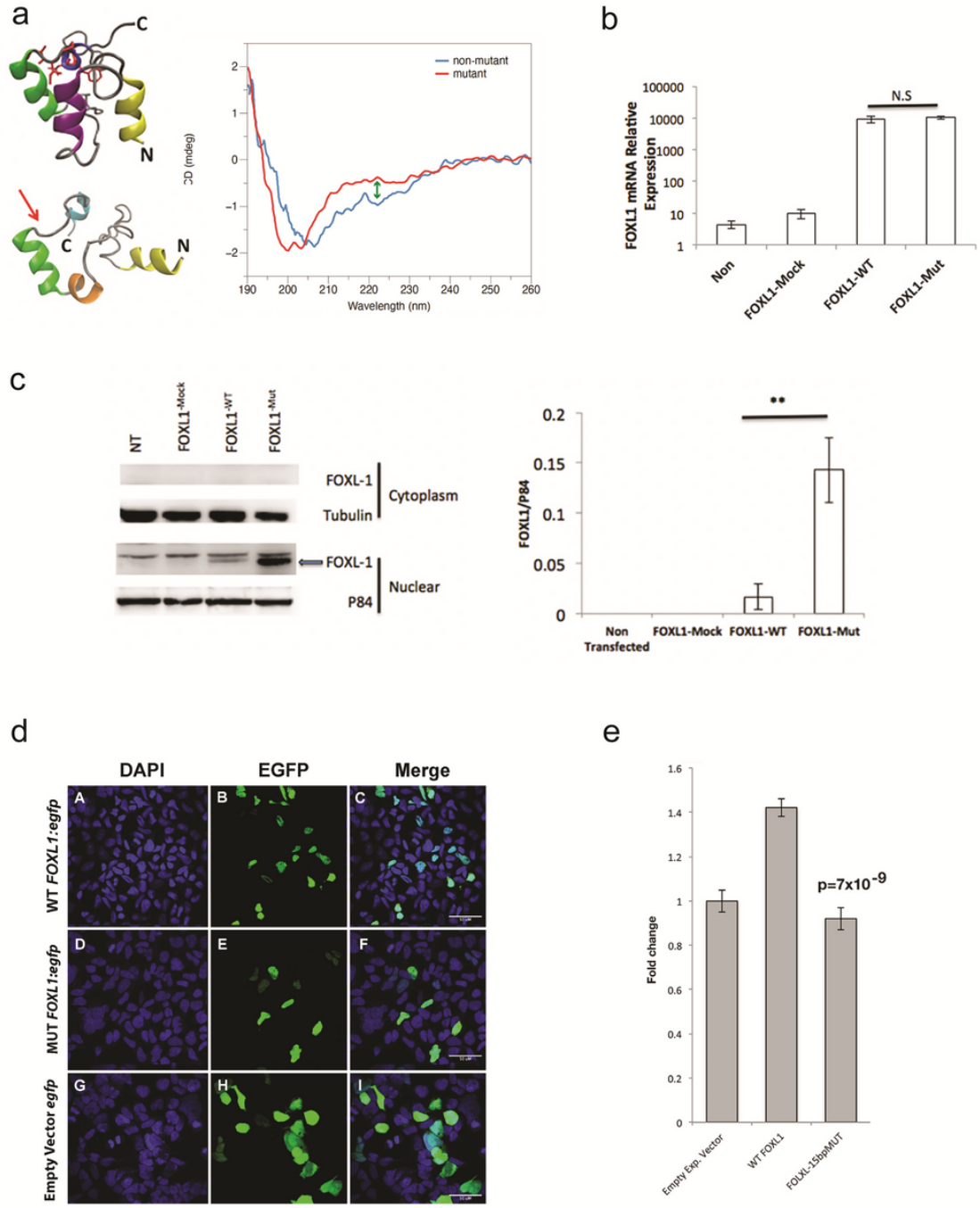

Figure 3

Structural and functional investigation of the 15-bp FOXL1 in-frame deletion. (a) Computational modeling displaying wildtype Foxl1 (top left) and misfolded Foxl1 (bottom left), the result of disrupting the hydrophobic core (arrow) producing a randomly coiled structure. Secondary structure (right) experimentally probed by circular dichroism (CD) in both wildtype and mutant Foxl1 produced recombinantly in E. coli. Note that wildtype Foxl1 appears to have twice as much helix as the mutant (arrow), the C-terminus of mutant Foxl1 is mostly random coil (48% of the helicity of wildtype). (b) In osteoblasts (hFOB1.19), both FOXL1 (hFOB-FOXL1-Mut) and the wildtype (hFOB-FOXL1) constructs express RNA to a high level (Non=non-transfection control; FOXL1-Mock=empty vector control). Bar graph represents the mean FOXL1 mRNA relative expression + SD of three independent experiments. GAPDH was used as an endogenous control. (c) In osteoblasts (hFOB1.19), cytoplasmic and nuclear extract proteins were prepared and immunoblotted using a FOXL1

antibody (ab83000) using αTubulin (DM1A+DM1B) and P84 (5E10) as cytoplasmic and nuclear loading controls, respectively (left). Protein levels assessed by Western blotting show significantly increased (**p<0.01) expression (right) of FOXL1 mutant (FOXL1-Mut) compared with FOXL1 wildtype (FOXL1-WT). FOXL1 levels were normalized to P84 and the average band intensity after normalization is presented in the bar graph. Error bars represent the ± SD of three independent experiments. (d) Expression of wildtype and mutant FOXL1:GFP fusion proteins in HEK293 cells. Transfection of constructs containing wildtype FOXL1;egfp fusion proteins demonstrates that wildtype FOXL1:egfp (panel B) localizes to the nucleus (panel A), as evidenced by their co-localization (panel C). Similarly, expression of mutant FOXL1:egfp fusion proteins (panel E) localizes to the nucleus (panel D) as evidenced by their colocalization (panel F). Expression of empty vector egfp [no FOXLQ ORF, (panel H)] localizes to both the nucleus (panel G) and cytoplasm, as evidences by egfp detection within and beyond the DAPI stain (panel I). (e) In HEK293 cells, transfection of constructs containing the wild-type FOXL1 ORF (WT FOXL1) increased transcription from the FOXL1 reporter by 42% over endogenous levels using a luciferase transcription assay. Transfection with the mutant ORF does not induce transcription from the reporter (FOXL1-15bpMUT), indicating a loss of transcriptional activity (p=7x10-9). Bar graph represents pixel intensity + SD of three independent experiments.

Supplementary Files

This is a list of supplementary files associated with this preprint. Click to download.

- SupplementaryFileHumanGeneticsSubmission.pdf